35th EPS Conference on Plasma Phys. Hersonissos, 9 - 13 June 2008 ECA Vol.**32D**, P-4.028 (2008)

Poloidal asymmetry of turbulent fluctuations in the torsatron TJ-K

M. Ramisch[1)], A. Köhn[1)], N. Mahdizadeh[2)], P. Manz[1)], U. Stroth[1)]

[1)] *Institut für Plasmaforschung, Universität Stuttgart, Germany*
[2)] *ABB Switzerland Ltd, Corporate Research, Switzerland*

Introduction: In toroidal fusion plasmas, poloidal $E \times B$ shear flows play an important role as a trigger mechanism for transitions into a regime of improved confinement [1]. The origin of these shear flows at spontaneous transitions is so far unclear. One candidate for the natural drive of such flows is the turbulent Reynolds stress [2]. Other theoretical works [3, 4] proposed poloidal inhomogeneity in, e.g., turbulent transport $\Gamma = < \widetilde{n}\widetilde{v}_r >_t$ as a possible origin of spontaneous $E \times B$ shear flows (Stringer spin up). $\widetilde{n}$ and $\widetilde{v}_r = \widetilde{E}_\theta / B$ are fluctuations in the density and the radial $E \times B$ velocity, respectively, with B the magnetic field strength. Indeed, ballooning effects due to magnetic-field curvature in toroidal geometry could cause in-out asymmetries in the fluctuations and related transport. In this work, the influence of magnetic-field curvature on drift-wave turbulence in the torsatron TJ-K [5] is studied. Fluctuations are measured with a multi-probe array on a complete circumference of an inner flux surface in the poloidal cross-section. The spatial structure of turbulent transport is analysed with a wavelet technique.

Experimental Setup: The experiments were conducted in the toroidally confined plasma of the torsatron TJ-K [6] with a major and a minor plasma radius of $R_0 = 0.6\,\mathrm{m}$ and $a = 0.1\,\mathrm{m}$, respectively. At a nominal magnetic field strengths in the range $B = 70$–$100\,\mathrm{mT}$, electron-cyclotron-resonance heating (ECRH) at 2.45 GHz is used for plasma generation. In the present experiment, the working gas was helium at a neutral gas pressure of $p_0 = 3 \times 10^{-5}\,\mathrm{mbar}$, a heating power of $P_{\mathrm{ECRH}} = 1.8\,\mathrm{kW}$ and a nominal magnetic field strength of $B = 72\,\mathrm{mT}$. The ions are cold ($T_i \lesssim 1\,\mathrm{eV}$).

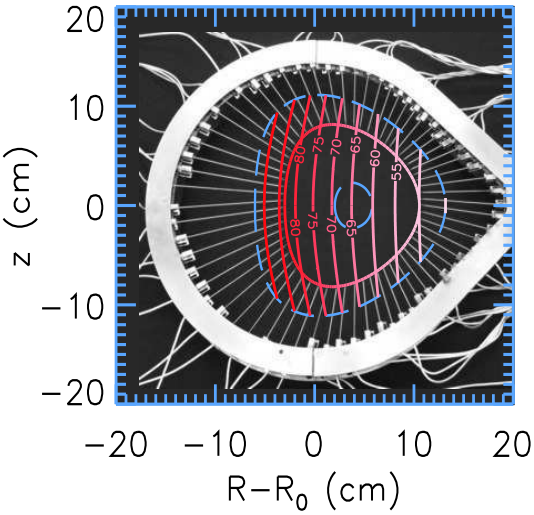

Fig. 1: Setup of the poloidal probe array. The separatrix and an inner flux surface are depicted as dashed lines. The color coded contours show the magnetic field strength B with the labels given in mT. That way, B is also indicated on the surface at the position of the probe tips.

A poloidal probe array consisting of 64 Langmuir probes was positioned inside the confinement region, where the density gradient is steepest. As shown in Fig. 1, the 64 probe tips are equally spaced at a distance $\Delta y \approx 7\,\mathrm{mm}$ on the full poloidal circumference of a flux surface with a triangular cross-section. For transport measurements [7], fluctuations in the floating potential ϕ_f and ion-saturation current $I_{\mathrm{i,sat}}$ are simultaneously acquired each from 32 probes in alternating order, i.e., $\widetilde{v}_{r,i} = -(\widetilde{\phi}_{f,i+1} - \widetilde{\phi}_{f,i-1})/(2\Delta y B_i)$, where $i = 1, 3, \ldots$ and B_i is calculated. Each signal consists of 1M values sampled at 1 MHz with 16-bit resolution. For all calculations, normalised fluctuations $e\phi/T_e$ and v/c_s are used, where $c_s = \sqrt{T_e/M_i}$ is the sound speed and $T_e = 13\,\mathrm{eV}$ is obtained from radial measurements with swept Langmuir probes. Density fluctuations are given by the ratio of fluctuations in $I_{\mathrm{i,sat}}$ and its local DC value, which in particular eliminates effects from varying probe tip sizes.

The spatial dependence of wave-number spectra is obtained by wavelet analysis (for details, see Ref. [8]). Wavelets have proven useful in time-frequency analysis of plasma turbulence [9]. In this work, the Morlet wavelet

$$\psi(y) = \pi^{1/4} \exp(i 2\pi y - y^2/2) \tag{1}$$

is used with the wavelet transform of a function $f(y)$ calculated according to

$$W_f(\delta, y_0) = \int f(y) \psi((y_0 - y)/\delta)/\sqrt{\delta}. \tag{2}$$

W_f is a complex-valued function of a scaling parameter (δ) and translation (y_0) in space. The result of the transformation is a local decomposition of the signal into a sinusoidal oscillation with Gaussian envelope dilated or contracted through δ. The scale δ can be associated with a wave number $k \approx 1/\delta$.

According to Ref. [10], the flux-surface averaged transport can be expressed in terms of the cross-power spectrum

$$\Gamma_{\mathrm{fl}} = \langle \widetilde{n}\widetilde{v} \rangle_{\mathrm{fl}} = \sum_j \sqrt{S_n(k_j) S_v(k_j)}\, \gamma(k_j) \cos(\varphi_{vn}(k_j)), \tag{3}$$

where S_f are the power spectra, γ is the cross-coherence and φ_{vn} the spatial phase relation of the fluctuations $\widetilde{v}$ and $\widetilde{n}$. Instead of using traditional Fourier components, the wavelet coefficients can be used [11] to calculate the different quantities in Eq. (3). Here, ensemble averages are taken over 1M realisations in time.

Fluctuation levels and net transport: In Fig. 2 (top), the relative fluctuation levels of the density and the potential as a function of the poloidal position y are shown. $y = 0$ corresponds to the outboard midplane. The values of both σ_n and σ_v are in the range 10 – 40 %. They are not constant on the flux surface and exhibit a similar structure. Local maxima are observed near the low-field side (LFS) at $y = 0.1$.

The net radial turbulent transport as shown in Fig. 2 (bottom) is calculated as a sample average of time windows of 1 ms length. A local maximum on the LFS is observed, which shows up more clearly than the maxima in the fluctuation levels. However, the maxima in both Γ and σ appear to be subject to a small shift of $\Delta y \approx 0.1$ with respect to $y = 0$. The shift shows into the direction of the poloidal $E \times B$ drift. In TJ-K, however, the poloidal $E \times B$ velocity is exceeded by the oppositely directed electron-diamagnetic drift, which determines the propagation of turbulent structures in the present drift-wave turbulence [12]. A propagation into $E \times B$ direction unaffected by the diamagnetic drift would rather be expected for interchange instabilities [13].

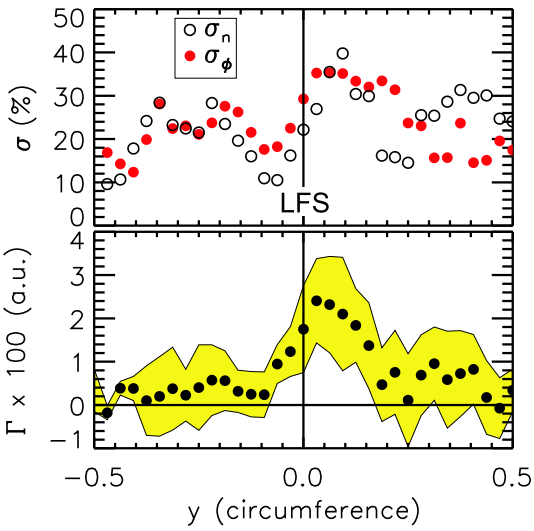

Fig. 2: Relative fluctuation levels (top) of density (○) and potential (●). Temporally averaged turbulent transport Γ (bottom) as a function of the poloidal position (in units of the full circumference, ccw). Zero is centred on the LFS. The scatter of Γ is shaded.

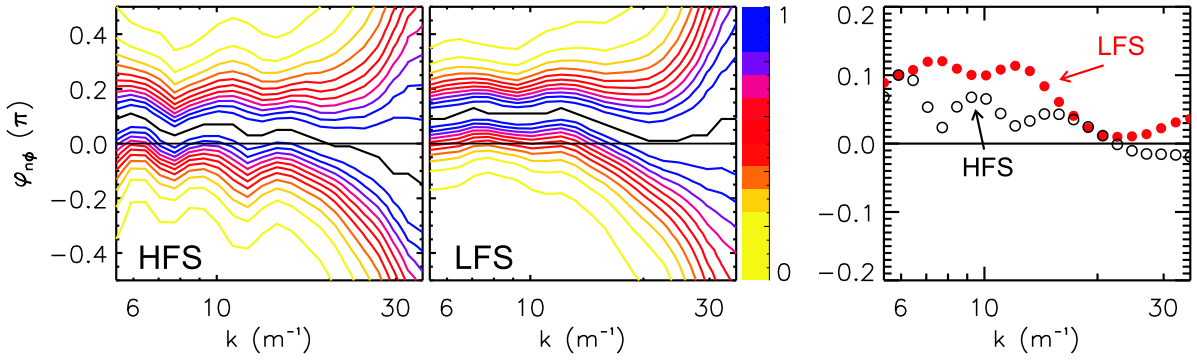

Fig. 3: *Contours of spatially averaged, normalised cross-phase histograms on the HFS (left) and the LFS (centre). For intermediate scales, the expectation value of $\varphi_{n\phi}$ is increased on the LFS (right).*

Wavelet cross-phase: In order to study the influence of magnetic-field curvature on drift-wave turbulence, the spatial cross-phase of density and potential fluctuations is examined in more detail. For each scale δ and each poloidal position, 1M realisations of $\varphi_{n\phi} = \arg(W_n W_\phi^*)$ are collected from the time series to calculate the PDF ($\phi_i = (\phi_{i-1} + \phi_{i+1})/2$ and the asterisk denotes the complex conjugate). PDFs from 7 positions are averaged separately on the high-field side (HFS) and on the LFS. The normalised histograms as a function of the wave number are shown as contour plots in Fig. 3. On the HFS and the LFS, the cross-phases are distributed in a narrow range around $\varphi_{n\phi} = 0$, which is indicative for drift-wave turbulence. Note that for the cross-phase $\varphi_{vn} = \pi/2 - \varphi_{n\phi}$. Towards smaller scales, the distributions broaden due to a decreasing coherence. For intermediate scales, the expectation values of $\varphi_{n\phi}$ are increased on the LFS, where maximum transport is observed. This difference might be a sign of change in the direction of curvature drive.

Wavelet transport: A more detailed picture of the turbulent transport is obtained from wavelet

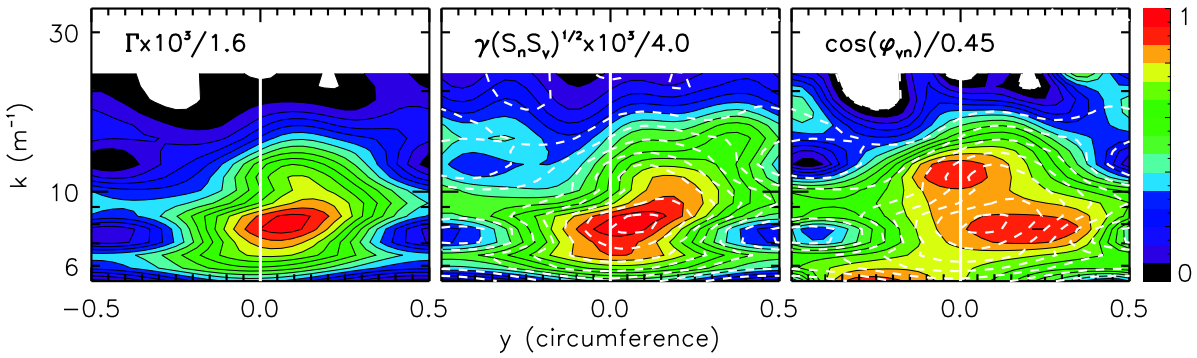

Fig. 4: *Wavelet decomposition of the turbulent transport according to Eq.* (3) *using* (2) *with the poloidal coordinate as in Fig. 2. Left: Poloidal dependence of $\Gamma_{\mathrm{fl},k}$. Centre: So called cross-amplitude spectrum. Right: Cosine of the cross-phase of $\widetilde{v}$ and $\widetilde{n}$. For comparison, the latter plots are overlaid with contours of $\Gamma_{\mathrm{fl},k}$. Regions with a coherence of less than* 0.5 *are omitted.*

analysis. The wavelet decomposition of the transport and its elements from Eq. 3 are shown in Fig. 4. In (y,k) space, a local maximum of transport is found at the same poloidal location on the LFS as in Fig. 2. For the present discharge, the maximum transport is observed at a wave number of $k = 8\,\mathrm{m}^{-1}$. On the HFS, the shape of the transport profile resembles those of the cross-amplitude spectrum and the cross-phase equally well. On the LFS, the transport appears

to be most similar to the cross-amplitude spectrum. However, also the cross-phase has its largest contribution in this region as already observed in Fig. 3. As a general trend, regions on the LFS with high fluctuation amplitudes tend to coincide with regions of larger cross-phases $\varphi_{n\phi}$. On the HFS, both the amplitudes and the cross-phases tend to be small. At the intermediate regions, large amplitudes but a reduced contribution to transport due to small cross-phases is observed (see, e.g., $(y, k) = (0.35, 14\,\mathrm{m}^{-1})$ in Fig. 4).

Summary: In order to get insight into the spatial structure of turbulent fluctuations on an inner flux surface of a toroidal plasma, measurements with a poloidal probe array were carried out in the torsatron TJ-K. A local maximum in fluctuation levels and net transport was found on the LFS of the magnetic configuration, where bad curvature gives rise to enhanced instability. In this region, wavelet analysis carried out on the data revealed an increase in the cross-phase $\varphi_{n\phi}$ of density and potential fluctuations. Though drift-wave turbulence is still dominant, the increase in $\varphi_{n\phi}$ might point to a contribution of curvature drive to the instability. On the LFS, high fluctuation power appears together with increased $\varphi_{n\phi}$ and on the HFS, low power together with lower $\varphi_{n\phi}$. However, the poloidal position of maximum transport is subject to a displacement from the LFS, which could be related to background $E \times B$ flow. Indeed, at magnetic-field reversal, the displacement changed sign (but also magnitude). The understanding of this effect is subject of future investigations and could be of special importance with regard to scrape-off layer transport or interpretations of results from single point measurements.

References

[1] K. Itoh and I. Sanae-I, Plasma Phys. Controll. Fusion **38**, 1 (1996).
[2] P. H. Diamond and Y. B. Kim, Phys. Fluids, B **3**, 1626 (1991).
[3] A. B. Hassam and T. M. Antonsen, Jr., Phys. Plasmas **1**, 337 (1994).
[4] A. G. Peeters, Phys. Plasmas **5**, 2399 (1998).
[5] U. Stroth *et al.*, Phys. Plasmas **11**, 2558 (2004).
[6] N. Krause *et al.*, Rev. Sci. Instrum. **73**, 3474 (2002).
[7] N. Mahdizadeh *et al.*, Plasma Phys. Controll. Fusion **47**, 569 (2005).
[8] M. Farge, Annu. Rev. Fluid Mech. **24**, 395 (1992).
[9] B. P. van Milligen, C. Hidalgo, and E. Sánchez, Phys. Rev. Lett. **74**, 395 (1995).
[10] E. J. Powers, Nucl. Fusion **14**, 749 (1974).
[11] B. P. van Milligen, in *Wavelets in Physics*, edited by J. C. van den Berg (Cambridge University Press, Cambridge, 2004), pp. 227 – 262.
[12] M. Ramisch, E. Häberle, N. Mahdizadeh, and U. Stroth, Plasma Sources Sci. Technol. **17**, 024007 (2008).
[13] D. L. Jassby, Phys. Fluids **15**, 1590 (1972).